ChemComm
Chemical Communications

Accepted Manuscript

This article can be cited before page numbers have been issued, to do this please use: R. Liu, Y. Luo, Y. Zheng, G. Zhang and C. Streb, *Chem. Commun.*, 2020, DOI: 10.1039/D0CC03758C.

ROYAL SOCIETY OF CHEMISTRY

rsc.li/chemcomm

View Article Online
DOI: 10.1039/D0CC03758C

COMMUNICATION

Polyoxometalate-like sub-nanometer molybdenum(VI)-oxo clusters for sensitive, selective and stable H_2O_2 sensing

Received 00th January 20xx,
Accepted 00th January 20xx

DOI: 10.1039/x0xx00000x

Rongji Liu,*[a,b] Yuyang Luo,[c] Yuanhao Zheng,[c] Guangjin Zhang,[b] Carsten Streb*[a,d]

Polyoxometalate-like molybdenum(VI)-oxo clusters ([Mo-oxo]$_n$, n = 1-20) deposited on high surface-area carbon are developed as a biosensor for non-enzymatic electrochemical H_2O_2 detection. The sensor exhibits excellent electrocatalytic performance with a low detection limit, wide linear range, excellent sensitivity and stability. The composite can be stably deposited on screen-printed electrodes which combine microlitre analyses, long shelf-life and re-usability.

Hydrogen peroxide (H_2O_2) is a well-known oxidant, bleaching agent and antiseptic, and is a key compound in pulp- and paper-bleaching, bio-medicine, environmental science and food industries.[1] However, due to its high reactivity, H_2O_2 holds potential hazards in technological and biological environments. To this end, the design of (bio)sensors which quantify H_2O_2 with high sensitivity, wide detection range and good selectivity is a major current research theme. In particular the design of enzyme-free electrochemical sensors offers significant advantages including low cost, high stability and long-term usage.[2]

This has led to the use of noble metals including monometallic Ag,[3,4] Au,[5,6] Pt[7] and Pd[8] based systems as well as bimetallic sensors,[9,10] which demonstrated high activity for electrochemical H_2O_2 sensing. However, the high costs of these metals has led to alternative solutions where metal-free conductive carbon based materials,[11,12] or transition metal oxides and sulphides,[13–19] have been used as low-cost H_2O_2 (bio)sensors. Despite this progress, there are still unsolved challenges relating to stability and selectivity. Thus, urgent work is required to translate progress in materials design into accessing advanced, technologically relevant H_2O_2 biosensor materials. One main challenge in the field is electrochemical sensitivity, *i.e.* accessing the maximum number of electrochemically active sites on a given electrode surface. To this end, single atom catalysts, metal clusters and metal oxide clusters have recently been studied as promising candidates for this task.[20–22] However, the development of noble-metal-free metal or metal oxide clusters for H_2O_2 biosensors is still challenging as many systems lack the sensitivity and long-term stability required for technological use.

One compound class which could offer access to designer materials for electrochemical sensors are polyoxometalates (POMs). POMs are early transition metal oxo clusters whose structure and electrochemistry can be tuned on the molecular level. This has led to their use as electrochemical (bio)sensors for the quantitative detection of H_2O_2 and other biomolecules.[23–27] However, in the bulk, POMs are typically insulators, so to make them amenable for electrochemical sensing, POMs have to be stably linked to electrically conductive substrates.[28–30] Major current challenges in POM-on-electrode deposition are the homogeneous and molecular distribution of POMs together with their mechanically and chemically stable linkage to prevent leaching under operation. In addition, simple deposition routes are urgently required to access scalable and technologically relevant composites.

Herein, for the first time, we demonstrate the use of polyoxomolybdate-like sub-nanometer molybdenum(VI)-oxo clusters ([Mo-oxo]$_n$, n = 1-20) supported on N, P-doped conductive mesoporous carbon as a highly efficient and highly stable enzyme-free H_2O_2 biosensor. Briefly, the composite (hereafter: **1**) was synthesized in a facile, scalable top-down route and has recently been reported by some of us as efficient oxygen reduction reaction catalyst (details see ESI).[31] The Mo loading of composite **1** is 10.4 wt% as determined by inductively coupled plasma optical emission spectroscopy (ICP-OES). Here, we prepared biosensor electrodes by loading **1** (0.3 mg cm^{-2} based on geometric surface area) onto a glassy carbon rotating disk electrode (RDE).

First, we examined the electrochemical response of **1** to different concentrations of H_2O_2. To this end, cyclic

[a] Institute of Inorganic Chemistry I, Ulm University, Ulm, 89081, Germany
E-mail: rongji.liu@uni-ulm.de, carsten.streb@uni-ulm.de.
[b] Institute of Process Engineering, Key Laboratory of Green Process and Engineering, Chinese Academy of Sciences, Beijing, 100190, China.
[c] School of Materials Science and Engineering, Tsinghua University, Beijing 100084, China.
[d] Helmholtz-Institute Ulm, Electrochemical Energy Conversion, Ulm, 89081, Germany.

† Footnotes relating to the title and/or authors should appear here.
Electronic Supplementary Information (ESI) available: details of any supplementary information available should be included here]. See DOI: 10.1039/x0xx00000x

voltammetry (CV) was performed using **1** deposited on a RDE as working electrode, a platinum foil as counter-electrode and saturated calomel electrode (SCE) as reference electrode (details see ESI). All studies were performed in aqueous solution containing 0.1 M aqueous phosphate buffer solution (PBS, pH 7.0) as electrolyte. As shown in Figure 1a, the H_2O_2-free electrolyte shows a typical double-layer capacitance characteristic. Increasing concentrations of H_2O_2 ($[H_2O_2]$ = 0 - 15 mM) result in increasing cathodic currents as well as a shift of the reduction peak potential to more negative values. The calibration curve (Fig. 1b) indicates that the peak current at -0.3 V *vs.* SCE increases linearly with the H_2O_2 concentration in the range studied. This allowed us to evaluate the use of the **1**-modified RDE as H_2O_2 biosensor. To this end, we examined the chronoamperometric (CA) response of the electrode to H_2O_2 at -0.3 V *vs*. SCE at 1600 rpm (Fig. 1c,d). Stepwise increase of the currents with increasing H_2O_2 concentration is observed with a current response of approx. 2 s. Even at low concentrations of 50 nM, the current increase is observed with a signal-to-noise ratio of ~3.5 (Fig. 1e). The calibration curve shown in Figure 1f indicates that the H_2O_2 sensor based on **1** exhibits a broad linear response range (LRR) from 50 µM to 5 mM, with the corresponding linear regression equation of *I* (mA) = -0.09604 $[H_2O_2]$ (mM) - 0.00227 (R^2=0.99). In the low concentration range (from 50 nM to 50 µM), the linear response is observed (Figure 1g) with the corresponding linear regression equation of *I* (µA) = - 0.12187 C (µM) − 2.21667 (R^2=0.999). Even in the very low concentration range (from 50 nM to 250 nM), a linear response is observed (inset of Figure 1h) with the corresponding linear regression equation of I (µA) = - 2.77808×10^{-4} C (nM) − 2.1933 (R^2=0.98).

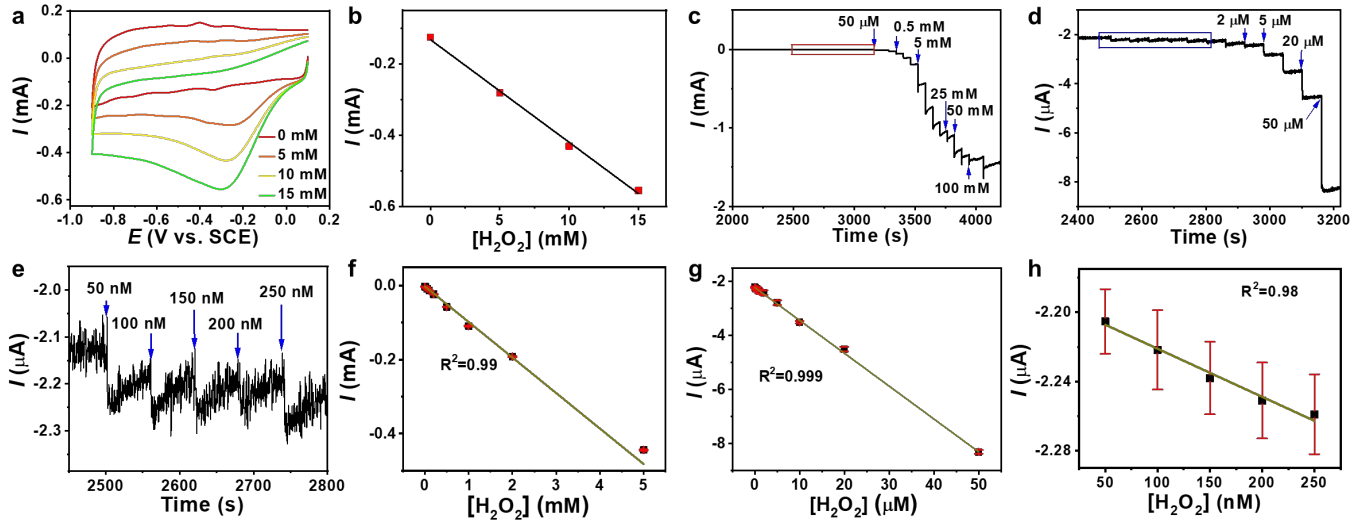

Fig. 1 Electrochemical study of the H_2O_2 detection by **1** deposited on a rotating disk electrode (RDE). a) CVs of the **1**-modified RDE (0.3 mg/cm^2) in 0.1 M aqueous PBS (pH = 7) at 50 mV s^{-1}; $[H_2O_2]$ = 0 to 15 mM. b) The corresponding calibration plot based on Fig. 1a, currents determined at -0.3 V *vs*. SCE. c) Chronoamperometric response of the **1**-modified RDE upon H_2O_2 addition (at -0.3 V *vs*. SCE in 0.1 M aqueous PBS, pH = 7). d) Magnified view of the red rectangular range in c. e) Magnified view of the blue rectangular range in d. f-h) The corresponding calibration plots extracted from c, d and e, respectively.

Next, we assessed the sensitivity and lower limit of detection (LOD) of the **1**-modified electrode as two key parameters of electrochemical sensors. For this, the following equations were used:[32]

$$\text{sensitivity} = \frac{k}{A}$$

$$\text{LOD} = \frac{S/N \cdot \sigma}{k}$$

where *k* is the linear regression slope, *A* is the geometric surface area of the working electrode, *σ* is the standard deviation of y-intercept of regression line, *S/N* is the signal-to-noise ratio and usually the value is 3. When applied to our test electrode, we obtained a sensitivity of 2.2 mA mM^{-1} cm^{-2} and a LOD of 0.23 µM. The H_2O_2 detection performance of **1** compares favourably with literature-known biosensors based on noble and non-noble metal/metal oxide clusters,[21,22,33–36] the detailed comparisons are shown in the ESI, Table S1. In particular, **1** shows a one of the broadest linear response ranges and a one of the lowest LOD, highlighting the viability of the proposed sensor composite design in **1**. It also compares favourably with a related composite based on hierarchically porous α-MoO_3 and graphene oxide, showing broader LRR, higher sensitivity and lower LOD.[16] For further comparison, we also studied two reference samples, i.e. **2** (nitrogen-doped mesoporous carbon (NMC)) and **3** (commercial MoO_3 nanoparticles physically mixed with NMC) as H_2O_2 sensors, experimental details see ESI. As shown in Figure S1, both samples showed lower sensing activity with more negative peak potential and lower current density than composite **1**.

For many technological applications, *e.g.* in biological systems, the sensor selectivity is another key factor. Particularly, sensors should show negligible response to other redox-active contaminants which could be present in the analyte matrix. To explore this behaviour, we exposed a 1-modified electrode to a range of model contaminants, i.e. methanol, ethanol, glucose and ascorbic acid (AA). Figure 2 shows the current

View Article Online
DOI: 10.1039/D0CC03758C

response of a **1**-modified electrode when these contaminants as well as H_2O_2 (50 µM each) were added to an aqueous PBS buffer (pH 7).[6] We note that the addition of H_2O_2 to the analyte leads to an instantaneous and significant amperometric response (~ 3 µA). Subsequent addition of ethanol, methanol, glucose and AA did not cause apparent amperometric changes, we only note a minor current decrease upon AA addition. In a sensor application, this could be clearly differentiated from the observed response to H_2O_2. Addition of a second aliquot of H_2O_2 at the final stage results in the identical response as observed for the first aliquot (~ 3 µA). In sum, this proof of concept demonstrates that **1** can act as interference-stable and selective (bio)sensor for H_2O_2.

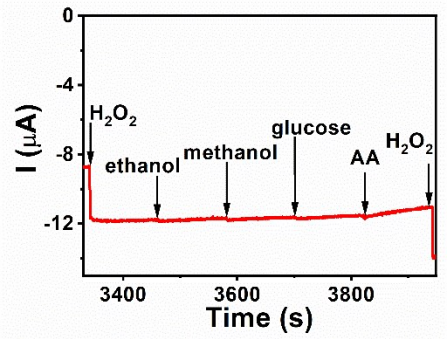

Fig.2 Selectivity of **1**. The contaminants ethanol, methanol, glucose, ascorbic acid (AA) and the H_2O_2 analyte (50 µM each) were added to an aqueous PBS buffer solution (pH 7), the working electrode was kept at a potential of -0.3 V vs SCE.

Next, we studied the charge transport and analyte diffusion behaviour of **1** using the Randles–Sevcik equation (eq. 1) to assess the H_2O_2 diffusion coefficient.[37]

$$I_p = 2.69 \times 10^5 \, n^{\frac{3}{2}} A D_{H2O2}^{\frac{1}{2}} [H_2O_2] \gamma^{\frac{1}{2}} \qquad \text{eq. 1}$$

where I_p is the peak current, n is the number of electrons transferred (here: 2), A is the geometric surface area of the electrode (cm^2), D_{H2O2} is the H_2O_2 diffusion coefficient (cm^2 s^{-1}), [H_2O_2] is the bulk concentration of the redox probe (mol cm^{-3}), and γ is the scan rate (V s^{-1}).

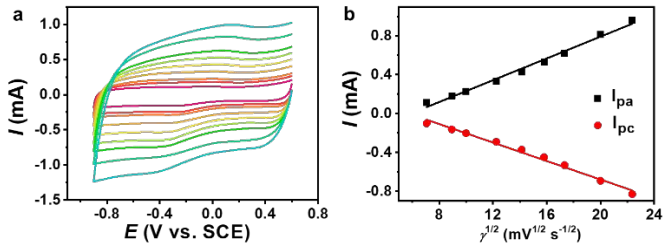

Fig. 3 H_2O_2 diffusion coefficient determination. a) CVs of the **1**-modified RDE electrode (loading (1): 0.3 mg/cm^2) in 0.1 M aqueous PBS buffer (pH = 7) containing 1 mM H_2O_2 at different scan rates (γ = 50, 80, 100, 150, 200, 250, 300, 400, and 500 mV s^{-1}). b) Plot of electrocatalytic anodic (I_{pa}) and cathodic peak current (I_{pc}) at 0 V *vs* $\gamma^{1/2}$.

To this end, CVs of the **1**-modified electrode at various scan-rates were recorded in a 0.1 M aqueous PBS (pH = 7) solution containing 1 mM H_2O_2. As shown in Figure 3a, both anodic and cathodic currents increase with increasing scan rates, and the current at 0 V *vs.* SCE were proportional to the square root of the scan rate (Figure 3b), indicating that the redox reaction of H_2O_2 on the electrode is diffusion-controlled. This allowed us to calculate the diffusion coefficient D_{H2O2} to be 3.4 × 10^{-4} cm^2 s^{-1}, which is higher than the reported PtNi NWs/rGO electrode (3.24 × 10^{-5} cm^2 s^{-1}),[38] which could indicate the faster H_2O_2 reduction in our molybdenum(VI)-oxo clusters system.

Finally, to demonstrate the technological readiness level and scalability of **1**-modified electrodes, we fabricated **1**-modified portable, disposable screen-printed electrodes (SPE, DropSens DRP-110 electrodes). The system uses carbon as working electrode (diameter = 4 mm, catalyst loading = 0.3 mg cm^{-2}) and counter electrode, while silver is used as reference electrode (details see ESI). Due to the compact size and electrode integration, microfluidic lab-on-a-chip applications could be envisaged.

As proof of principle, we performed CV and CA measurements (Figure S2 and S3) using 50 µL of aqueous H_2O_2 solution ([H_2O_2] = 0 - 100 mM) deposited SPE surface. The electrodes showed fast response times (~ 2 s) and high stability for H_2O_2 sensing. Long-term durability and reusability tests demonstrate that the identical SPE showed similar sensing performance after storage in air for 2 months after the initial test (Figure S4).

In conclusion, we demonstrate the first example of sub-nanometre Mo-oxo clusters deposited on conductive porous carbon as a versatile H_2O_2 sensor suitable for technological deployment, *e.g.* when deposited on mass-produced screen-printed electrodes. The sensor shows high stability and selectivity, is resistant against many common interfering contaminants and can be re-used. The work therefore lays the foundation for the development of this new materials class for electrochemical sensor development.

Conflicts of interest

There are no conflicts to declare.

Acknowledgements

Ulm University and the Helmholtz Gemeinschaft (HGF) are gratefully acknowledged for financial support. R.L. acknowledges the Alexander-von-Humboldt-Foundation for a postdoctoral fellowship (1186323). C.S. gratefully acknowledge the Deutsche Forschungsgemeinschaft DFG for financial support (STR1164/12). G.Z. acknowledges the National Natural Science Foundation of China (U1662121) and the Youth Innovation Promotion Association of the Chinese Academy of Sciences. G.Z. and C.S. acknowledge support by the CAS President's International Fellowship Initiative.

Notes and references

1 A. K. M. Kafi, G. Wu and A. Chen, *Biosens. Bioelectron.*, 2008, **24**, 566–571.
2 S. Chakraborty and C. Retna Raj, *Biosens. Bioelectron.*, 2009, **24**, 3264–3268.
3 G. Chang, Y. Luo, W. Lu, X. Qin, A. M. Asiri, A. O. Al-Youbi

and X. Sun, *Catal. Sci. Technol.*, 2012, **2**, 800–806.
4 B. Ma, C. Kong, X. Hu, K. Liu, Q. Huang, J. Lv, W. Lu, X. Zhang, Z. Yang and S. Yang, *Biosens. Bioelectron.*, 2018, **106**, 29–36.
5 J. Ju and W. Chen, *Anal. Chem.*, 2015, **87**, 1903–1910.
6 R. Liu, S. Li, X. Yu, G. Zhang, S. Zhang, J. Yao, B. Keita, L. Nadjo and L. Zhi, *Small*, 2012, **8**, 1398–1406.
7 S. Guo, D. Wen, Y. Zhai, S. Dong and E. Wang, *ACS Nano*, 2010, **4**, 3959–3968.
8 W. Xue, X. Bo, M. Zhou and L. Guo, *J. Electroanal. Chem.*, 2016, **781**, 204–211.
9 K. J. Chen, K. Chandrasekara Pillai, J. Rick, C. J. Pan, S. H. Wang, C. C. Liu and B. J. Hwang, *Biosens. Bioelectron.*, 2012, **33**, 120–127.
10 T. Zhang, Y. Xing, Y. Song, Y. Gu, X. Yan, N. Lu, H. Liu, Z. Xu, H. Xu, Z. Zhang and M. Yang, *Anal. Chem.*, 2019, **91**, 10589–10595.
11 T. Kuila, S. Bose, P. Khanra, A. K. Mishra, N. H. Kim and J. H. Lee, *Biosens. Bioelectron.*, 2011, **26**, 4637–4648.
12 Z. Wang and Z. Dai, *Nanoscale*, 2015, **7**, 6420–6431.
13 W. Jia, M. Guo, Z. Zheng, T. Yu, E. G. Rodriguez, Y. Wang and Y. Lei, *J. Electroanal. Chem.*, 2009, **625**, 27–32.
14 Y. Li, Y. Zhong, Y. Zhang, W. Weng and S. Li, *Sensors Actuators, B Chem.*, 2015, **206**, 735–743.
15 A. K. Dutta, S. K. Maji, D. N. Srivastava, A. Mondal, P. Biswas, P. Paul and B. Adhikary, *ACS Appl. Mater. Interfaces*, 2012, **4**, 1919–1927.
16 B. Li, H. Y. Song, Z. P. Deng, L. H. Huo and S. Gao, *Sensors Actuators, B Chem.*, 2019, **288**, 641–648.
17 T. Wang, H. Zhu, J. Zhuo, Z. Zhu, P. Papakonstantinou, G. Lubarsky, J. Lin and M. Li, *Anal. Chem.*, 2013, **85**, 10289–10295.
18 H. Du, X. Zhang, Z. Liu and F. Qu, *Chem. Commun.*, 2019, **55**, 9653–9656.
19 Z. Wei, Z. Hai, M. K. Akbari, D. Qi, K. Xing, Q. Zhao, F. Verpoort, J. Hu, L. Hyde and S. Zhuiykov, *Sensors Actuators, B Chem.*, 2018, **262**, 334–344.
20 H. Hanfeng, M. Junjie, H. Yunhu, W. Fei, Z. Meining, W. Dingsheng, M. Lanqun and L. Yadong, *Sci. China Chem.*, 2019, **625**.
21 X. Niu, C. Chen, H. Zhao, Y. Chai and M. Lan, *Biosens. Bioelectron.*, 2012, **36**, 262–266.
22 C. Zhang, L. Li, J. Ju and W. Chen, *Electrochim. Acta*, 2016, **210**, 181–189.
23 C. Sun, X. Chen, J. Xu, M. Wei, J. Wang, X. Mi, X. Wang, Y. Wu and Y. Liu, *J. Mater. Chem. A*, 2013, **1**, 4699–4705.
24 Y. Zhang, X. Bo, A. Nsabimana, A. Munyentwali, C. Han, M. Li and L. Guo, *Biosens. Bioelectron.*, 2015, **66**, 191–197.
25 B. Haghighi, H. Hamidi and L. Gorton, *Electrochim. Acta*, 2010, **55**, 4750–4757.
26 L. Kang, H. Ma, Y. Yu, H. Pang, Y. Song and D. Zhang, *Sensors Actuators, B Chem.*, 2013, **177**, 270–278.
27 M. H. Yang, D. S. Kim, T. J. Lee, S. J. Lee, K. G. Lee and B. G. Choi, *J. Colloid Interface Sci.*, 2016, **468**, 51–56.
28 Y. Ji, L. Huang, J. Hu, C. Streb and Y. Song, *Energy Environ. Sci.*, 2015, **8**, 776–789.
29 S. Herrmann, C. Ritchie and C. Streb, *Dalton Trans.*, 2015, **44**, 7092–7104.
30 A. S. Cherevan, S. P. Nandan, I. Roger, R. Liu, C. Streb and D. Eder, *Adv. Sci.*, 2020, **7**, 1903511.
31 R. Liu, K. Cao, A. H. Clark, P. Lu, M. Anjass, J. Biskupek, U. Kaiser, G. Zhang and C. Streb, *Chem. Sci.*, 2020, **11**, 1043–1051.
32 N. Yusoff, P. Rameshkumar, M. S. Mehmood, A. Pandikumar, H. W. Lee and N. M. Huang, *Biosens. Bioelectron.*, 2017, **87**, 1020–1028.
33 M. J. Wei, J. Q. Fu, B. Li, K. Z. Shao, H. Y. Zang, X. H. Wang and Z. M. Su, *New J. Chem.*, 2019, **43**, 13430–13436.
34 G. Yue, S. Li, W. Liu, F. Ding, P. Zou, X. Wang, Q. Zhao and H. Rao, *Sensors Actuators, B Chem.*, 2019, **287**, 408–415.
35 C. Hegarty, S. McKillop, T. Dooher, D. Dixon and J. Davis, *IEEE Sensors Lett.*, 2019, **3**, 1–4.
36 F. Wen, Y. Dong, L. Feng, S. Wang, S. Zhang and X. Zhang, *Anal. Chem.*, 2011, **83**, 1193–1196.
37 A. J. Bard and L. R. Faulkner, *Electrochemical Methods: Fundamentals and Applications*, John Wiley & Sons, New York, 2000.
38 Y. Sun, M. Luo, Y. Qin, S. Zhu, Y. Li, N. Xu, X. Meng, Q. Ren, L. Wang and S. Guo, *ACS Appl. Mater. Interfaces*, 2017, **9**, 34715–34721.

View Article Online
DOI: 10.1039/D0CC03758C

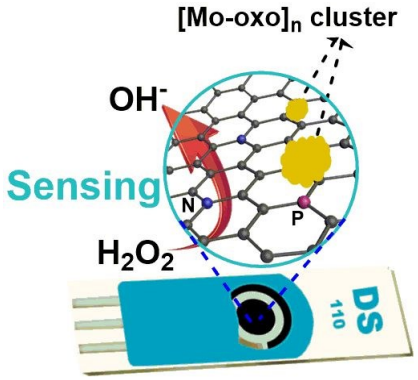

Polyoxometalate-like sub-nanometer molybdenum(VI)-oxo clusters supported on mesoporous carbon are stably deposited on glassy carbon and screen-printed electrodes suitable for selective, sensitive and stable H_2O_2 sensing.